Side-jump effect in paramagnetic amorphous metals

K. Rhie and D. G. Naugle

Department of Physics, Texas A&M University, College Station, Texas 77843-4242

Beom-hoan O and J. T. Markert

Department of Physics, University of Texas at Austin, Austin, Texas 78712

(Received 1 February 1993; revised manuscript received 10 May 1993)

A systematic study of the resistivity (ρ), the Hall coefficients (R_H), and the magnetic susceptibilities (χ) of the Zr-based paramagnetic amorphous alloys suggests a self-consistent explanation for the frequently observed positive values of R_H that is based on the side-jump effect. Measurements for χ, R_H, and ρ of $(Zr_{0.64}Cu_{0.36})_{1-x}Al_x$ and χ for $(Zr_{0.50}Ni_{0.50})_{1-x}Al_x$ alloys are presented. The odd behavior of the Hall coefficients of these alloys and the anomalous positive Hall coefficients of paramagnetic Zr-based amorphous alloys can be accounted for in terms of the enhanced spin-orbit interaction, which produces the side-jump effect.

I. INTRODUCTION

Many amorphous metallic alloys have positive Hall coefficients (R_H). Positive values of R_H are found for some amorphous rare-earth-based alloys, weak ferromagnetic alloys, early-transition-metal (ETM)–late-transition-metal (LTM) alloys, and ETM–simple-metal alloys. The positive R_H and its magnetic-field dependence for the amorphous dilute Fe alloys and rare-earth metal-based alloys are explained with the side-jump effect.[1,2] However, the applicability to the paramagnetic alloys remains controversial.

For ETM-LTM and ETM–simple-metal amorphous alloys, the value of R_H increases with increasing ETM content and even changes its sign from negative to positive for some alloy systems. Amorphous La-Al (Ref. 3), La-Ga (Ref. 4), Y-Al (Ref. 5), Zr-Ni (Ref. 6), Zr-Co (Ref. 7), Zr-Cu (Ref. 8), Hf-Cu (Ref. 8), and Ti-Cu (Ref. 8) are examples. The value of R_H also increases as the LTM is substituted by one further to the right side of the periodic table. The Zr-based alloys illustrate this behavior particularly well, e.g., Zr-Co, Zr-Ni, and Zr-Cu. Furthermore, the addition of a simple metal such as Al or Ga into a binary ETM-LTM alloys increases the value of R_H (Refs. 9–11) up to some relatively high concentration beyond which addition of the simple metal decreases R_H.

The positive values of R_H of these paramagnetic binary and pseudobinary alloys are quite puzzling. One of the first theoretical explanations of the crossover from negative to positive values with increasing ETM for nonmagnetic amorphous alloys was s-d hybridization. According to theory, the s band and d band are hybridized to make a negative dispersion relation near the Fermi level, with a corresponding negative group velocity, which gives the positive Hall coefficient. In this model R_H is given[12] by

$$R_H^{sd} = \frac{-\alpha[dN_s(\varepsilon)/d\varepsilon]|_{\varepsilon=\varepsilon_F}}{2eN_s(\varepsilon_F)^2,} \qquad (1.1)$$

where α is a constant of order unity and $N_s(\varepsilon)$ is the density of states of the hybridized s states. A perturbative calculation with a single s band and a single d band indicated that s-d hybridization indeed could produce a positive Hall coefficient when the Fermi level lies in an appropriate region in the d band.[13] In this perturbation calculation, the negative dispersion was gradually washed out with the dilution so that the positive Hall coefficient of Zr-Cu would become negative when the Cu concentration is large enough. More sophisticated approaches show more structure in the value of R_H as a function of energy than the perturbation calculation.[12,14] The result of our former work, however, indicates some difficulties in explaining the positive Hall coefficients of $(Zr_{0.64}Ni_{0.36})_{1-x}Al_x$ and $(Zr_{0.50}Ni_{0.50})_{1-x}Al_x$ alloys.[10,11] Recently, very precise measurements of the temperature dependence of R_H have been reported.[15,16] Schulte et al.[15] proposed that both the positive value of R_H and the negative temperature dependence of R_H beyond that expected from the electron-electron interaction can be understood in terms of s-d hybridization. Both effects are attributed to the static and thermal broadening of the electron spectral function. Rhie, Naugle, and Bhatnager[10] pointed out that the model had an inconsistency in explaining the temperature dependence of R_H when it is negative, and they also tried to explain the temperature dependence in terms of the side-jump effect.

The side-jump effect introduced by Berger[17] provided a reasonable explanation for the anomalous Hall effect of ferromagnetic[1,2] and nearly ferromagnetic materials, as mentioned above. Recently, a large temperature dependence of R_H has been reported for paramagnetic Zr-Fe alloys near the composition boundary for the ferromagnetic regime.[18,19] The temperature dependence of R_H follows that of the susceptibility. Even though the origin of the temperature dependence of the Pauli susceptibility for these alloys is still not clear,[20–22] these experiments strongly suggest that the side-jump effect plays an important role in determining R_H for the paramagnetic alloys.

<u>48</u>   5973

The first purely paramagnetic alloys with composition well away from the magnetic regime whose R_H was interpreted in terms of the side-jump effect were the $(Zr_{0.64}Ni_{0.36})_{1-x}Al_x$ (Ref. 10) and $(Zr_{0.50}Ni_{0.50})_{1-x}Al_x$ (Ref. 11) alloys. The increase of R_H, which even resulted in a change in the sign from negative to positive for the $(Zr_{0.50}Ni_{0.50})_{1-x}Al_x$ series, produced by adding the simple metal Al was interpreted as a result of the side-jump effect which would be enhanced by an increase of the sample resistivity.[11]

The Zr-Cu binary alloy system has been frequently cited as a good example for the s-d hybridization model because the increase of R_H with increasing Zr concentration for Zr-Cu alloys could be reproduced by a suitable choice of the parameters for the potential of hybridization.[12] However, since data for the similar ternary alloy, $(Zr_{0.64}Ni_{0.36})_{1-x}Al_x$ has been interpreted in terms of the side-jump mechanism, amorphous $(Zr_{0.64}Cu_{0.36})_{1-x}Al_x$ alloys are therefore an attractive choice for study with the goal of separating these two effects.

In this paper, we report the results of Hall effect and the magnetic susceptibility measurement for $(Zr_{0.64}Cu_{0.36})_{1-x}Al_x$ alloys and the susceptibility of $(Zr_{0.50}Ni_{0.50})_{1-x}Al_x$ alloys. Then, we point out that the positive contribution to R_H from the side-jump effect in these purely paramagnetic amorphous alloys is large enough, due to the large resistivity and the spin-orbit interaction of $4d$ electrons of transition-metal alloys, to overcome the Lorentz term (R_H^0). We will indicate how the side-jump mechanism can explain qualitatively the composition dependence of R_H for a wide range of amorphous Zr-based alloys. The odd composition dependence of R_H for $(Zr_{0.64}Cu_{0.36})_{1-x}Al_x$ alloys will be discussed in detail.

II. EXPERIMENT

The $Zr_{0.64}Cu_{0.36}$ and $Zr_{0.50}Ni_{0.50}$ ingots were prepared by arc melting appropriate amounts of 99.996% pure Cu, 99.9% pure Ni, and 99.6% pure Zr in an Ar atmosphere. The simple metal, 99.999% pure Al, was added to the ingots to reach a proper concentration and again arc melted. The ribbons were melt spun in a single roller melt spinner at a wheel speed of about 30 m/sec. The typical sample width was 3 mm with thicknesses of 18 to 23 μm.

A conventional dc, five terminal method was used for the Hall measurements. Fine copper wires (No. 40) were spot welded at the edges of the sample. The magnetic field applied was from -1 to 1 T, and the Hall voltage was measured with a Keithley 181 nanovoltmeter. R_H values of several batches of each alloy concentration, melt spun at different times, were measured to check for sample aging, but the difference between samples of the same composition was within the measurement error of 0.5×10^{-11} (m^3/C).

The resistances of the samples were measured with a four-probe method. In order to increase the accuracy of the measurement, 2–3 in. long ribbon was used with fine, spot-welded copper wires. The resistivity (ρ) was calculated directly from the resistance, mass, density, length of the ribbon, and the distance between the voltage probes.

The accuracy of the resistivity is better than 5%.

The magnetic susceptibilities of the samples were measured at room temperature using a superconducting quantum interference device magnetometer and a magnetic-field strength of 1 T. The sample was cut into 0.6–0.8-cm lengths by the fold-cutting method, in order to rule out the possibility of introduction of any magnetic impurity. A bunch of the short pieces were stacked into a 1-cm-long gelatin capsule and mounted in the magnetometer. The diamagnetic susceptibility of the capsule was measured separately, and subtracted from the raw data. At least 40 mg of sample was required to overcome the diamagnetic signal of the capsule, because the paramagnetic signal of the samples was so small. Typically, 70–100 mg of each sample was used. The absolute accuracy of magnetization measurements is better than one percent. $(Zr_{0.64}Cu_{0.36})_{1-x}Al_x$ alloys showed a small nonlinearity with H, but it will be discussed in other work.[23]

III. RESULTS

A. $(Zr_{0.64}Cu_{0.36})_{1-x}Al_x$ alloys

The value of R_H for $Zr_{0.64}Cu_{0.36}$ was 5.3×10^{-11} (m^3/C), very close to the recently reported value of 5.15×10^{-11} (m^3/C) for $Zr_{0.60}Cu_{0.40}$,[24] but smaller than the values reported earlier for similar alloys, 6.6×10^{-11} (m^3/C) for $Zr_{0.70}Cu_{0.30}$ and 6.1×10^{-11} (m^3/C) for $Zr_{0.60}Cu_{0.40}$.[25] The behavior of R_H for $(Zr_{0.64}Cu_{0.36})_{1-x}Al_x$ is rather curious. The values remained constant at about 5.0×10^{-11} (m^3/C) up to $x = 0.10$, then suddenly jumped to 8.9×10^{-11} (m^3/C) at $x = 0.15$. Several batches of this composition showed the same result within the error of 0.5×10^{-11} (m^3/C). The value of R_H decreased again to 6.8×10^{-11} (m^3/C) at $x = 0.20$. See Fig. 1.

The resistivity (ρ) of $(Zr_{0.64}Cu_{0.36})_{1-x}Al_x$ alloys increased with x. The value of ρ at $x = 0$ is comparable to the previously measured data of 166 $\mu\Omega$ cm (Ref. 26) and 167 $\mu\Omega$ cm (Ref. 27). The abnormally high resistivity of $x = 0.05$ shown in Fig. 1 may be due to aging since this sample was quenched several months before the measurement of ρ. At this composition, the magnetic susceptibility data (Fig. 2) also show some disagreement with the generally decreasing tendency of χ with x. The increase of the resistivity is about 10% with the addition of 20 at. % of Al into the binary $Cu_{0.36}Zr_{0.64}$ alloy. The total magnetic susceptibility of the alloy decreased 15% with the addition of 20 at. % of Al, but the valence susceptibility increased with x up to $x = 0.10$, then decreased to the value without Al upon further addition of Al. The reason for the initial decrease of the Pauli susceptibility is that the decrease of the Van Vleck susceptibility, which is proportional to the Zr content, is faster than the decrease of total magnetic susceptibility. The valence (Pauli) susceptibility was calculated from the following equation,

$$\chi_v = \chi - \chi_{vv}^{Zr} C_{Zr} - \sum_i \chi_{dia}^i C_i , \qquad (3.1)$$
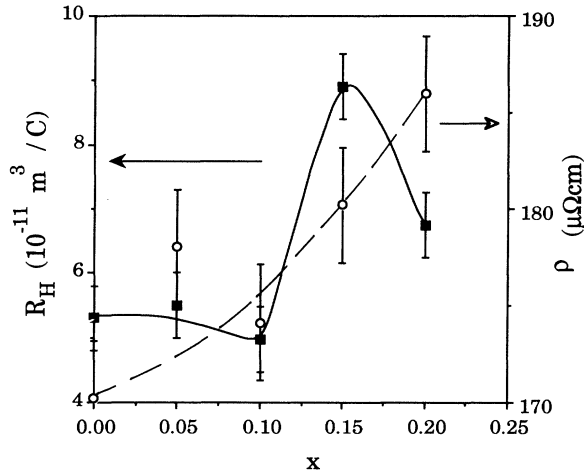
where i stands for Zr, Cu, and Al. Figure 2 illustrates the

FIG. 1. The Hall coefficient (filled squares) and resistivity ρ (open circles) as a function of Al content for $(Zr_{0.64}Cu_{0.36})_{1-x}Al_x$ alloys. The solid and broken lines are guides showing the trend of the data. The value of R_H increases to reach a maximum at $x = 0.15$, then decreases again. Except for the value at $x = 0.05$, ρ increases smoothly with the Al content.

total magnetic susceptibility (χ) and the valence susceptibility (χ_v) with Al content. Values of χ_{vv}^{Zr} were determined from NMR measurements by Eifert, Elschner, and Buschow.[28] The density of the alloys decreased monotonically with the Al content as expected.

B. $(Zr_{0.50}Ni_{0.50})_{1-x}Al_x$ alloys

For $(Zr_{0.50}Ni_{0.50})_{1-x}Al_x$ alloys, our measurements of R_H, ρ, and density have been reported previously.[11] R_H of the alloys showed a change of sign from negative to positive as Al is added. In this work we report values of
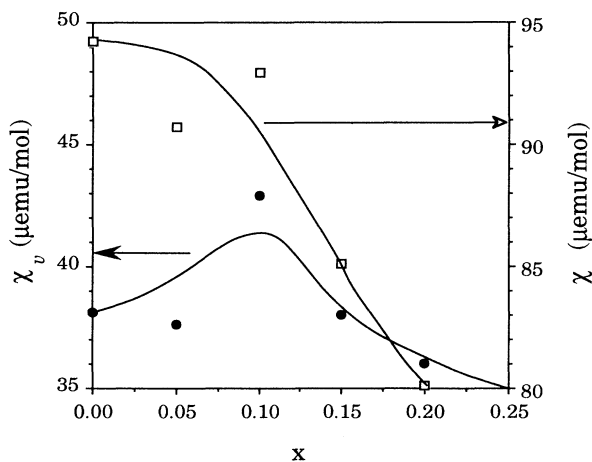

FIG. 2. Total magnetic susceptibility χ (open squares) and valence magnetic susceptibility χ_v (solid circles) vs Al content x for $(Zr_{0.64}Cu_{0.36})_{1-x}Al_x$ alloys. Values of χ decrease with x, but χ_v exhibits a maximum at $x = 0.10$.
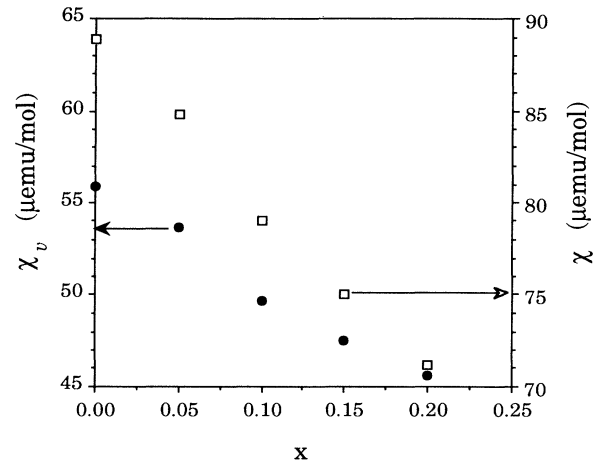

FIG. 3. χ (open squares) and χ_v (solid circles) vs Al content x for $(Zr_{0.50}Ni_{0.50})_{1-x}Al_x$ alloys. Both quantities decrease with Al content.

the magnetic susceptibility of these alloys. The magnetic susceptibility for $Zr_{0.50}Ni_{0.50}$ is 88.9 μemu/mol, which is comparable to that previously reported, 91 μemu/mol.[26] When the simple metal Al is introduced, the susceptibility decreased monotonically, but more rapidly than for the $(Zr_{0.67}Ni_{0.33})_{1-x}Al_x$ alloy (see Fig. 3). This provides an important clue to predict the tendency of R_H of other ternary alloys, and it will be discussed below.

IV. DISCUSSION

For ETM-LTM alloys and ETM–simple-metal amorphous alloys, the sign of R_H changes from negative to positive as the concentration of ETM is increased. Furthermore, R_H increases as the LTM element is substituted by one further to the right side of the periodic table. The Zr-based alloys Zr-Cu, Zr-Ni, Zr-Co, and Zr-Fe illustrate this behavior particularly well. We also note that, according to ultraviolet photoemission spectroscopy (UPS) measurements,[29,30] the density of states for the Zr d band increases with the Zr content, and the binding energy E_b of the LTM peak increases as the element is substituted by one further to the right side of the periodic table. This coincidence indicates that the anomalous positive portion of the R_H is strongly correlated with the density of states and nature of the dominant d states at the Fermi level.

We briefly summarize the results from the theory of the side-jump effect, then apply it to explain R_H for the binary and pseudobinary Zr-based alloys.

A. Side-jump effect

When an electron wave packet is scattered by an ion, the wave packet experiences the spin-orbit interaction. The scattered wave function for each angular momentum quantum number has been calculated by including the spin-orbit interaction term in the Hamiltonian by Smit.[31] In addition to scattering, each electron wave picks up a phase shift proportional to the spin-orbit interaction.

The phase shift is antisymmetric about the incident axis of the electron wave packet. As a result, the net effect is to shift the center of mass of the electron wave packet in the transverse direction without changing its momentum. The side jump literally means this shift of the center of mass.[1,17] If the Hamiltonian has antisymmetric matrix elements, then the scattering is skewed and the momentum is not conserved. But we do not discuss this skew scattering in this work.

Berger[17] suggested that the shift of the center of mass or the side-jump effect gives rise to an anomalous Hall effect. Fivaz demonstrated that a conducting electron in a crystal (or in the presence of short-range order) sees an enhanced spin-orbit interaction due to the crystal field.[32] Berger and Bergmann[1] calculated the effective spin-orbit coupling parameter for $3d$ electrons based on the Fivaz Hamiltonian and found it was about 10^4 times larger than that of free electrons. They gave the following expression for the side-jump contribution to the Hall resistivity:

$$\rho_H^{SJ} = \rho^2 \sigma_{xy}^{SJ}$$
$$= \sum_i \frac{2\rho^2 N_i q_i^2}{\hbar} \lambda_{SO}^{SJ} \langle S_z \rangle \ , \tag{4.1}$$

with

$$\lambda_{SO}^{SJ} = \sum_n \frac{|\langle n|\mathbf{L}|0\rangle|^2}{E_n - \varepsilon_F} Il^2 A_{SO} \ , \tag{4.2}$$

where i denotes carrier type, q_i denotes charge of i-type carrier, λ_{SO}^{SJ} denotes the effective spin-orbit parameter, A_{SO} is the atomic spin-orbit parameter, I is the overlap integral, and l is the distance between the scatterers.

Please note that ferromagnetism is not required for the side-jump mechanism to contribute an anomalous term to R_H. Only a spin polarization is needed. If the magnetic field is strong enough, the expectation value $\langle S_z \rangle$ for conduction electrons will be close to S_z for ferromagnetic materials. In contrast, that expectation value for paramagnetic materials is field dependent and usually quite small. For the case of paramagnetic metals, $\langle S_z \rangle$ can be written as[19]

$$\langle S_z \rangle = \frac{\chi_v B_z}{N_d \mu_B \mu_0} \ , \tag{4.3}$$

where χ_v is the Pauli paramagnetic susceptibility, which is sometimes written as the Stoner enhanced Pauli paramagnetism

$$\chi_v = \frac{\chi_p}{1-I} \ ,$$

where I is the Stoner enhancement parameter.

Since ρ_H is linearly dependent on B_z, the measured Hall coefficient will be given for the paramagnetic case by

$$R_H = R_H^0 + R_H^S \chi_v \ , \tag{4.4}$$

$$R_H^S = \frac{2e^2}{\hbar g \mu_0 \mu_B} \lambda_{SO}^{SJ} \rho^2 \ ,$$

where R_H^0 is due to Lorentz force, and $R_H^S \chi_v$ comes from the side-jump effect.

B. Side-jump effect in binary Zr-LTM materials (LTM = Co, Ni or Cu)

For the estimation of R_H^0, one might suggest that charge carriers are contributed $2e$ by Zr, $0.6e$ by Ni, $0.5e$ by Co, and $1e$ by Cu. The values for Zr and Cu are taken from Ref. 33, and those for Ni and Co are calculated from the liquid-state Hall coefficients[34] of the elements. With this assumption, one can write

$$R_H^S \chi_v = R_H^{measured} + \frac{1}{n|e|}$$
$$= R_H^{measured} + \frac{A}{|e|N_A d(e/a)}, \tag{4.5}$$

where e/a is the average number of charge carriers per atom, A is the average molecular weight, N_A is the Avogadro number, and d is the density.

To test these ideas, $\Delta R_H = R_H - R_H^0 = R_H^S \chi_v$, determined for numerous amorphous Zr-LTM alloys, is plotted against $\chi_v \rho^2$ in Fig. 4. Values of the parameters for each concentration are compiled in Table I. The slope of each imaginary line passing through the origin and any data point should be just a constant times λ_{SO}^{SJ}, according to Eq. (4.4). Alloys chosen for Zr-Ni and Zr-Co are in the paramagnetic regime, well away from the ferromagnetic transition which occurs at about 65% of Co and 83% of Ni in LTM-Zr. The data points for all these alloys fall approximately on a straight line. We offer no ex-
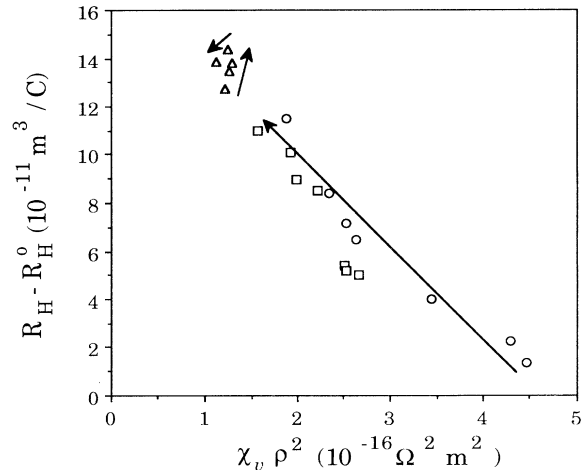
FIG. 4. $\Delta R_H = (R_H - R_H^0) = R_H^S \chi_v$ vs $\chi_v \rho^2$ for binary Zr-Cu (triangles), Zr-Ni (squares), and Zr-Co (circles) alloys. The empirical linearity of the data in this figure is unexpected, and is not understood. The arrows indicate the direction of increasing Zr content. Note that the volume susceptibility χ_v is in SI units, i.e., dimensionless. In accordance with Eq. (4.4), the slope of each imaginary line passing through the origin and any data point should be a constant times λ_{SO}^{SJ}, as formulated in Eq. (4.6). The general behavior of the data points is explained in terms of density of states near the Fermi level.

planation for the fact that all of the data for this diverse group of Zr-based alloys follow such a trend.

Besides the linearity of the data, the plot of $R_H - R_H^0$ against $\chi_v \rho^2$ for Zr-LTM alloys shows the following features: (1) ΔR_H, and consequently $R_H^S \chi_v$, increases with Zr content for Zr-Ni and Zr-Co, but shows little variation with Zr-Cu, (2) for the same Zr content, $R_H^S \chi_v$ of Zr-LTM alloys increases in the order Co→Ni→Cu,

and (3) $R_H^S \chi_v$ is always positive for these alloys over the composition ranges shown.

We argue below that this general behavior originates from the change of λ_{SO}^{SJ} caused by the variation of density of states among the different Zr-LTM amorphous alloys. Thus we use values of $R_H^S \chi_v$ and $\chi_v \rho^2$ to calculate an "experimental" value of λ_{SO}^{SJ} in terms of the free-electron spin-orbit parameter λ_{SO}^{free}, where

TABLE I. Values of the Hall coefficient for Zr-LTM binary alloys due to side-jump effect $R_H^S \chi_v$ and the enhanced spin-orbit interaction coefficients λ_{SO}^{SJ} together with the value of $\chi_v \rho^2$ in SI units. Values of the Lorentz term R_H^0 were subtracted from the measured Hall coefficient R_H, to find the value of $R_H^S \chi_v$. The molar valence susceptibility χ_v was transformed to a volume susceptibility in the value of $\chi_v \rho^2$, because the spin polarization is proportional to the volume susceptibility. Mass density, resistivity ρ, and the sum of valence susceptibility χ_v with Van Vleck susceptibility χ_{vv}, which were used for these analysis, are also listed.

x	Density[a] (g/cm^3)	ρ[a] $(\mu\Omega\,cm)$	R_H^0[a] $(10^{-11}m^3/C)$	$\chi_v + \chi_{vv}$[a] $(\mu emu/mol)$	χ_v $(\mu emu/mol)$	$\chi_v \rho^2$ $(10^{-16}\,\Omega^2 m^2)$	R_H $(10^{-11}\,m^3/C)$	$R_H^S \chi_v$ $(10^{-11}\,m^3/C)$	$10^{-4}\lambda_{SO}^{SJ}/\lambda_{SO}^{free}$
				$Zr_x Cu_{1-x}$ alloys					
0.75	6.85	158.2	−7.29	133.70	47.45	1.21			
0.72	6.87[b]	159.0[b]	−7.31	129.80[b]	46.42	1.21	5.40[c]	12.71	5.37
0.70	6.89	162.0	−7.33	125.90	45.40	1.24			
0.67	6.95	165.0	−7.33	118.90	41.85	1.21			
0.65	7.00	166.0	−7.31	116.00	41.25	1.23			
0.60	7.07	169.5	−7.34	108.50	39.50	1.26	6.10[d]	13.44	5.47
0.55	7.14	171.5	−7.37	96.64	33.39	1.12	6.50[c]	13.87	6.35
0.50	7.25	177.0	−7.37	91.40	33.90	1.25	7.00[d]	14.37	5.88
0.45	7.34	180.0	−7.40	84.47	32.72	1.29			
0.40	7.37	183.0	−7.49	77.00	31.00	1.29	6.30[c]	13.79	5.48
0.30		175.0[c]	−7.64				4.60[c]	12.24	
0.10							−5.10[c]		
				$Zr_x Ni_{1-x}$ alloys					
0.80	6.80	160.0	−7.50	152.80	60.80	1.57	3.51[e]	11.01	3.59
0.76	6.88	165.5	−7.55	150.90	63.50	1.80			
0.71	6.93	169.0	−7.67	145.10	63.45	1.93	2.39[e]	10.06	2.67
0.67	7.06	168.0	−7.68	140.70	63.65	1.98	1.27[e]	8.95	2.31
0.63	7.10	173.0	−7.78	136.80	63.77	2.15			
0.60	7.17	176.0	−7.85	131.00	62.00	2.21	0.67[e]	8.52	1.97
0.55	7.32	185.0	−7.91	124.35	61.10	2.51	−2.48[e]	5.43	1.11
0.50	7.50	183.5	−7.96	117.04	59.54	2.52	−2.80[e]	5.16	1.05
0.45	7.63	180.0	−8.10	110.80	59.05	2.50			
0.40	7.81	175.5	−8.20	107.15	61.15	2.58			
0.36	7.96	172.0	−8.30	104.70	63.30	2.66	−3.30[f]	5.00	0.96
0.33	8.05	168.0	−8.41	101.10	63.15	2.60			
				$Zr_x Co_{1-x}$ alloys					
0.80	6.80	162.00	−7.60	162.80	70.80	1.87	3.88[f]	11.48	3.14
0.75	7.00	164.00	−7.57	156.20	69.95	1.99			
0.70	7.12	173.00	−7.65	151.60	71.10	2.34	0.73[f]	8.38	1.84
0.67	7.20	176.00	−7.70	149.80	72.75	2.53	−0.55[f]	7.15	1.45
0.65	7.35	175.00	−7.64	149.10	74.35	2.63	−1.17[f]	6.47	1.26
0.60	7.40	180.00	−7.83	158.60	89.60	3.45	−3.81[f]	4.02	0.60
0.55	7.63	183.00	−7.86	166.00	102.75	4.30	−5.61[f]	2.25	0.27
0.53	7.70	176.00	−7.90	174.00	113.05	4.46	−6.56[f]	1.34	0.15

[a]Reference 26.
[b]Interpolated from the values in Ref. 26.
[c]Reference 8.
[d]Reference 25.
[e]Reference 6.
[f]Reference 7.

$$\lambda_{SO}^{free}=\tfrac{1}{2}\alpha^2 a_0^2 \ ,$$

$$\lambda_{SO}^{SJ}=\left\{\left|\frac{\Delta R_H}{\chi_v\rho^2}\right|\right\}\frac{\hbar g\mu_0\mu_B}{2e^2} \tag{4.6}$$

$$=5.1\times10^{-2}\frac{\Delta R_H}{\chi_v\rho^2}\lambda_{SO}^{free}\quad\text{(in SI units.)}$$

For example, for $Zr_{0.50}Ni_{0.50}$, $\Delta R_H=6.85\times10^{-11}$ m^3/C, $\chi_v\rho^2=2.42\times10^{-16}$ Ω^2 m^2 yields $\lambda_{SO}^{SJ}=1.44\times10^4\lambda_{SO}^{free}$, which is in satisfactory agreement with the estimate of 10^4 λ_{SO}^{free} by Berger and Bergmann for $3d$ electrons.[1] Some authors substitute the summation term in Eq. (4.2) with the Van Vleck susceptibility. Such an equalization may be acceptable in order to estimate the gross magnitude of λ_{SO}^{SJ}. However, such a substitution is improper for

consideration of the variation of λ_{SO}^{SJ}, because in the equation for χ_{vv},

$$\chi_{vv}=\sum_{E_m>E_n}\frac{|\langle m|\mathbf{L}|n\rangle|^2}{E_m-E_n} \tag{4.7}$$

the summation always produces a positive value, while the summation in the Eq. (4.2) is over all states, both filled and unfilled, and in principle, can produce a positive or a negative value depending on the band structure.

Values of λ_{SO}^{SJ} determined in the fashion of Eq. (4.6) are tabulated for the different Zr-LTM alloys in Table I and for the pseudobinaries in Table II. In terms of the values of λ_{SO}^{SJ} the observed behavior of $R_H^S\chi_v$ can be restated as (1) λ_{SO}^{SJ} increases with Zr content for Zr-Co and Zr-Ni, the variation with Zr-Cu is much smaller than for Zr-Co

TABLE II. Same information for some Zr-LTM-Al pseudobinary alloys as given in Table I. The x denotes Al content. χ_v was evaluated from χ, the total susceptibility.

x	Density (g/cm^3)	ρ ($\mu\Omega$ cm)	R_H^0 (10^{-11} m^3/C)	χ (μemu/mol)	χ_v (μemu/mol)	$\chi_v\rho^2$ (10^{-16} Ω^2 m^2)	R_H (10^{-11} m^3/C)	$R_H^S\chi_v$ (10^{-11} m^3/C)	$10^{-4}\lambda_{SO}^{SJ}/\lambda_{SO}^{free}$
				$(Zr_{0.64}Ni_{0.36})_{1-x}Al_x$ Alloys[a]					
0.00	7.25	178.0	−7.59	117.0[b]	66.6	2.42	0.9	8.5	1.81
0.05	7.10	186.0	−7.14	115.0[b]	67.4	2.70	1.2	8.3	1.58
0.10	6.96	193.0	−6.71	109.0[b]	64.1	2.81	2.5	9.2	1.68
0.15	6.73	205.0	−6.41	103.0[b]	60.8	3.02	4.2	10.6	1.80
0.20	6.53	214.0	−6.09	98.0[b]	58.5	3.19	6.7	12.8	2.06
0.25	6.21	229.0	−5.92	93.0[b]	56.2	3.47	8.4	14.3	2.11
				$(Zr_{0.50}Ni_{0.50})_{1-x}Al_x$ Alloys[c]					
0.00	7.46	186.0	−8.01	88.9[d]	55.9	2.42	−1.2	6.8	1.45
0.05	7.37	194.0	−7.36	84.8[d]	53.6	2.58	−1.0	6.4	1.26
0.10	7.19	203.2	−6.88	79.0[d]	49.7	2.64	0.0	6.9	1.33
0.15	6.83	210.3	−6.61	75.0[d]	47.6	2.66	0.6	7.2	1.39
0.20	6.77	214.9	−6.10	71.2[d]	45.6	2.74	1.1	7.2	1.34
				$(Zr_{0.33}Ni_{0.67})_{1-x}Al_x$ Alloys[e]					
0.00	7.48	189.0	−9.06	101.1[g]	63.2	3.05	−4.3	4.8	0.80
0.10	7.43	198.0	−7.24		56.7[f]	3.18	−3.5	3.7	0.58
0.20	6.96[f]	210.0	−6.25		51.7[f]	3.27	−2.6	3.6	0.56
0.30		280.0					−1.4		
0.50		239.0					0.9		
0.65		227.0					3.4		
0.70	3.74	209.0	−4.55				0.0	4.6	
0.75	3.06	172.0	−5.06				−1.8	3.3	
0.80	3.33	177.0	−4.22				−1.9	2.4	
0.85	2.99	95.0	−4.26				−3.9	0.3	
				$(Zr_{0.64}Cu_{0.36})_{1-x}Al_x$ Alloys[d]					
0.00	6.97	170.2	−7.36	94.3	38.1	1.22	5.3	12.7	5.33
0.05	6.84	178.0	−6.97	90.7	37.6	1.33	5.5	12.5	4.79
0.10	6.75	174.1	−6.55	93.0	42.9	1.48	5.0	11.5	3.98
0.15	6.53	180.2	−6.29	85.1	38.0	1.41	8.9	15.2	5.50
0.20	6.35	186.0	−6.01	80.1	36.0	1.44	6.8	12.8	4.54

[a]Reference 10.
[b]Reference 37.
[c]Reference 11.
[d]Present work.
[e]Reference 40.
[f]Extrapolated from $(Zr_{0.67}Ni_{0.33})_{1-x}Al_x$ and $(Zr_{0.50}Ni_{0.50})_{1-x}Al_x$ alloys.
[g]The value of $\chi_v+\chi_{vv}$, Reference 26.

or Zr-Ni, (2) for the same Zr content, λ_{SO}^{SJ} of Zr-LTM increases in the order of Co→Ni→Cu, and (3) λ_{SO}^{SJ} is always positive for these alloys over the composition ranges shown.

In accordance with Eq. (4.2) the value of λ_{SO}^{SJ} should be determined by four factors, the atomic spin-orbit parameter A_{SO}, the overlap integral I, the square of the distance between the scatterers l^2, and sum over states.

We argue that the dominant factor determining the change of λ_{SO}^{SJ} will be the sum over filled and unfilled states, since the unfilled states will provide a positive contribution and the filled states will provide a negative contribution. Due to the energy denominator the states near the Fermi energy will contribute more strongly to λ_{SO}^{SJ}. In this sum states for Zr would be weighted by A_{SO} for Zr, while those for the LTM would be weighted by A_{SO} for that particular element. For the alloys considered, A_{SO} for Zr should be appreciably larger, but nevertheless the contribution to the sum for the LTM component cannot be ignored.

In this approach, λ_{SO}^{SJ} can be broken into two parts, one for the ETM d states and one for the LTM d states where each part would be weighted by appropriate $IA_{SO}l^2$. For each component we argue that the change in I is roughly canceled by the change in l^2 as the composition is changed. Thus λ_{SO}^{SJ} is given by

$$\lambda_{SO}^{SJ} = \{Id^2 A_{SO}\Sigma\}_{ETM} + \{Id^2 A_{SO}\Sigma\}_{LTM}$$

and   (4.8)

$$\Sigma_i = \int_{-\infty}^{\infty} \frac{|\langle \varepsilon|L|0\rangle|_i^2}{\varepsilon} g_i(\varepsilon)d\varepsilon ,$$

where $i = $ ETM, LTM and $g_i(\varepsilon)$ is the density of states. A theoretical band calculation could provide a prediction of the variation of λ_{SO}^{SJ} for comparison with experiments. Unfortunately, no systematic calculation of the band structure which provides the matrix elements and density of states needed to estimate λ_{SO}^{SJ} for these alloys is available. If we ignore the energy dependence of the matrix elements, λ_{SO}^{SJ} will be determined primarily by the location of the Fermi energy ($\varepsilon = 0$) relative to the two d bands and the density of states for the ETM and LTM components.

Several reports of UPS spectra[29,30,35] and a soft x-ray emission spectra study[36] made it possible to correlate λ_{SO}^{SJ} with the qualitative variation of the density of states with alloy composition. The qualitative variation of the density of states for Zr-LTM alloys provides an explanation of the rules (1)–(3) for λ_{SO}^{SJ} deduced above from experiment. To facilitate the discussion of this explanation, we reproduce in Fig. 5 the UPS spectra which reflect the variation of the density of states below the Fermi energy for typical Zr-LTM amorphous alloys. In all of these alloys the Fermi energy lies in the lower half of the Zr d band and the LTM d band is centered below the Fermi energy by the binding energy, E_b. The unfilled Zr d states above ε_F are, of course, not reflected in the spectra of Fig. 5.

The first rule can be explained by the fact that as the Zr concentration is increased Σ_{Zr} becomes larger in magnitude, while Σ_{LTM} becomes smaller in magnitude. Note
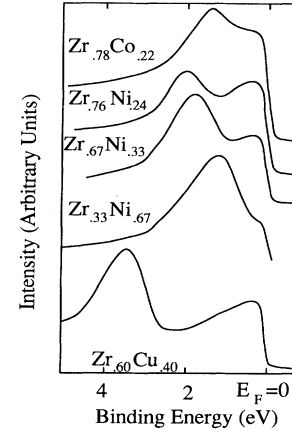

FIG. 5. UPS spectra (Refs. 29 and 30) for Zr-rich Zr-LTM alloys. Note that the location of LTM peak E_b shifts to a larger binding energy in the order of Zr-Co, Zr-Ni, and Zr-Cu, while the Zr peak is located above the Fermi energy ε_F so that λ_{SO}^{SJ} increases in the same order at a fixed LTM concentration.

that, because ε_F is located in the lower half of the Zr d band, Σ_{Zr} will be positive, but Σ_{LTM} will be negative because the center of the LTM d band is below ε_F; consequently, λ_{SO}^{SJ} increases with Zr content. For Co and Ni the density of states near ε_F is significantly larger than for Cu, i.e., E_b for Cu is significantly larger and less composition dependent than E_b for Co or Ni.[29] Thus, the negative contribution from Σ_{LTM} will show a much stronger variation with composition for Co and Ni than will Σ_{Cu} because of the $1/\varepsilon$ term. This variation is enhanced by the increase in LTM binding energy for Ni and Co with the increase in Zr content as seen in Fig. 5. Since almost all of the d states for Cu are well below ε_F, λ_{SO}^{SJ} will not vary rapidly with composition for Zr-Cu alloys, in agreement with Fig. 4.

The second rule follows from the fact that E_b increases in the order Co→Ni→Cu. Thus at a fixed composition, although Σ_{Zr} will change only slightly as a function of LTM, Σ_{LTM} (which is negative) will decrease significantly in the order Co→Ni→Cu. Consequently, λ_{SO}^{SJ} is expected to increase for fixed composition in the order Co→Ni→Cu, again in agreement with the data of Fig. 4.

The reason for the third rule is simply that ε_F lies in the lower half of the Zr $4d$ band; consequently, Σ_{Zr} is positive. Furthermore, at least for the alloys displayed in Fig. 4, $(l^2 IA_{SO}\Sigma)_{LTM}$ is less in magnitude than $(l^2 IA_{SO}\Sigma)_{Zr}$. At very high LTM concentration this rule would be expected to fail, but, perhaps primarily because A_{SO}^{Zr} is expected to be appreciably larger than A_{SO}^{LTM} for these particular alloys, the failure is not observed for the alloys listed in Table I.

C. $(Zr_{0.64}Ni_{0.36})_{1-x}Al_x$, $(Zr_{0.50}Ni_{0.50})_{1-x}Al_x$, and $(Zr_{0.33}Ni_{0.67})_{1-x}Al_x$ alloys

So far we have argued that λ_{SO}^{SJ} of Zr-based LTM alloys is in good agreement with the value predicted by Berger

and Bergmann.[1] Furthermore, we have shown that the qualitative variation of the density of states with composition can explain the variation of λ_{SO}^{SJ} (and consequently R_H) for a wide range of binary Zr-LTM alloys. But the most dramatic argument for the existence of a side-jump effect in paramagnetic amorphous alloys must be the ternary $(Zr_{0.64}Ni_{0.36})_{1-x}Al_x$ system.

For binary Ni-Zr alloys, R_H increased with the Zr concentration. However, the value of R_H of $(Zr_{0.64}Ni_{0.36})_{1-x}Al_x$ increased dramatically with the Al composition, x.[10-11] A similar result is reported for $(Zr_{0.67}Ni_{0.33})_{1-x}Al_x$ alloys.[37] Values of $\Delta R_H = R_H^S \chi_v$ for the $(Zr_{0.64}Ni_{0.36})_{1-x}Al_x$, calculated as described above with the assumption that Al contributes $3e$ per atom, versus $\chi_v\rho^2$ are shown in Fig. 6. Values of χ_v are taken from Ref. 37 for $(Zr_{0.67}Ni_{0.33})_{1-x}Al_x$ alloys. The behavior of $R_H^S \chi_v$ in these alloys is quite different from that of the binary Zr-Ni alloys. For this system $R_H^S \chi_v$ and $\chi_v\rho^2$ both increase appreciably with x over the range $0 < x < 0.30$. The value of λ_{SO}^{SJ} inferred from these data remains constant within about 10% over this range of x. This is quite reasonable, since the addition of the simple metal Al is not expected to change the relative position of the Zr and Ni d bands, but only reduce the overall density of states. Indeed this is confirmed by UPS measurements,[38] which show that the relative shape of the density of states is unchanged with addition of up to 15 at. % of Al and that the overall density of states near ε_F is lowered by about 9% (C_P data[36] shows a 19% decrease for the same Al content). Therefore one might assume that the maximum deviation of the λ_{SO}^{SJ} with Al doping to be less than 20% based on Eq. (4.8). The overall change of λ_{SO}^{SJ} for $(Zr_{0.64}Ni_{0.36})_{1-x}Al_x$ alloys is much smaller,

however, than those of the binary Zr-Ni or Zr-Co alloys, and to a good approximation, λ_{SO}^{SJ} remains constant. The straight line through the triangles in Fig. 6 indicates this average value of λ_{SO}^{SJ}.

With the values of χ_v from Fig. 3 and previous measurements of R_H and ρ,[11] a similar analysis can be made for $(Zr_{0.50}Ni_{0.50})_{1-x}Al_x$ alloys, also shown in Fig. 6. As previously reported, R_H values of $(Zr_{0.50}Ni_{0.50})_{1-x}Al_x$ alloys increase with x and change sign at $x = 0.10$. The increase in both R_H and $\chi_v\rho^2$ is very small, however. These data also lie very close to a straight line through the origin, and it is obvious that the $(Zr_{0.50}Ni_{0.50})_{1-x}Al_x$ alloys also have a constant λ_{SO}^{SJ} for the same reason as in the case of $(Zr_{0.64}Ni_{0.36})_{1-x}Al_x$ alloys. One can think of two reasons for the slower increase of R_H in the $(Zr_{0.50}Ni_{0.50})_{1-x}Al_x$ alloys. First, the λ_{SO}^{SJ} of the equicontent binary alloy is less than that of the Zr-rich binary alloy. Second, but more important, is that the reduction of the valence susceptibility of $(Zr_{0.50}Ni_{0.50})_{1-x}Al_x$ with x is much larger than that of $(Zr_{0.64}Ni_{0.36})_{1-x}Al_x$ alloys, so that the decrease of χ_v effectively cancels out the smaller increase of ρ^2 with x.

The larger decrease of χ_v for the higher Ni content pseudobinary alloy may result from the following trend. The χ_v of the Zr-Cu alloys decreases with Cu content, because the Zr electron states are diluted by the simple metal Cu. However, the χ_v of Zr-Co alloys increases with Co content[26,39] because, we suppose, the Stoner enhancement due to the Co more than compensates the reduction of Zr electron states. Zr-Ni alloys stand between those two extremes, so that the χ_v of this binary paramagnetic alloys has an almost constant value throughout the whole concentration range. When a simple metal such as Al or a metalloid such as H or Si is added to the binary Zr-Ni alloy, both the Zr electron state and the Stoner enhancement are diluted by the simple metal or metalloid. Generally the dilution of the Stoner enhancement is much faster. Therefore, the reduction of χ_v for $(Zr_{0.50}Ni_{0.50})_{1-x}Al_x$ is faster than that of $(Zr_{0.64}Ni_{0.36})_{1-x}Al_x$. By analogy, we expect that the change of $\chi_v\rho^2$ is small for Ni-rich alloys, because the rapid reduction rate of χ_v should offset the increase of ρ^2 is small for Ni-rich alloys, because the rapid reduction rate of χ_v should offset the increase of ρ^2 for the Ni-rich pseudobinary alloys. Therefore, the smaller increase of R_H for $(Zr_{0.33}Ni_{0.67})_{1-x}Al_x$,[40] compared to $(Zr_{0.50}Ni_{0.50})_{1-x}Al_x$ is justified. Also, even a reduction of R_H for $(Zr_{0.40}Ni_{0.60})_{1-x}H_x$ (Ref. 24) may be possible. Data for $(Zr_{0.33}Ni_{0.67})_{1-x}Al_x$ alloys with χ_v extrapolated from values from $(Zr_{0.67}Ni_{0.33})_{1-x}Al_x$ and $(Zr_{0.50}Ni_{0.50})_{1-x}Al_x$ are also shown in Fig. 6.
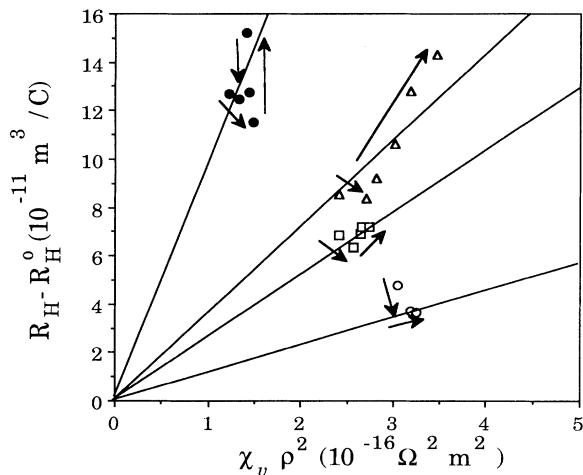

FIG. 6. $\Delta R_H = (R_H - R_H^0) = R_H^S \chi_v$ vs $\chi_v\rho^2$ for pseudobinary $(Zr_{0.64}Ni_{0.36})_{1-x}Al_x$ (triangles), $(Zr_{0.50}Ni_{0.50})_{1-x}Al_x$ (squares), $(Zr_{0.33}Ni_{0.67})_{1-x}Al_x$ (open circles), and $(Zr_{0.64}Cu_{0.36})_{1-x}Al_x$ (filled circles) alloys. The arrows show the direction of increasing Al. Note the lines pass through the origin approximately, indicating an almost constant λ_{SO}^{SJ} for these pseudobinary alloy series. The increase of $R_H^S \chi_v$ with Al content of Zr-rich alloys is larger than that of Zr-poor alloys.

D. $(Zr_{0.64}Cu_{0.36})_{1-x}Al_x$ alloys

Addition of Al increases R_H for values of x up to 0.15 in the same fashion as for $(Zr_{0.64}Ni_{0.36})_{1-x}Al_x$ alloys.[10] At $x = 0.20$, the value of R_H decreases. This decrease is most likely related to a change in the character of the d states at ε_F. When the simple-metal content is large enough, especially when Zr is diluted with Al, the states

at the Fermi level in the alloy tend to change gradually from the d-electron dominant states to sp-electron dominant states, i.e., the Hall coefficient decreases with Al content and then eventually reaches a negative value associated with amorphous or liquid Al. As an example, the R_H values of $Zr_{0.50-x}Cu_{0.50}Al_x$ alloys[41] increase up to $x = 0.10$, then decrease to reach a negative value approaching that of liquid Al. Such limiting behavior of the anomalous Hall coefficient at high Al concentration is found in several other ETM-LTM−based pseudobinary alloys also. Melt-spun or evaporated $(Ti_{0.76}Ni_{0.24})_{1-x}Al_x$ (Ref. 42), $(Ti_{0.67}Ni_{0.33})_{1-x}Al_x$ (Ref. 40), and $(Zr_{0.33}Ni_{0.67})_{1-x}Al_x$ (Ref. 40) samples showed an initial increase of R_H with x, but at higher Al concentrations, R_H began to decrease with x and eventually reached a negative value characteristic of the disordered simple metal.

In the framework of the side-jump effect, we have neglected the s-d hybridization[12−14] contribution. The success in explaining R_H in terms of the side jump alone suggests that the effect of s-d hybridization is weaker than had been expected, or the hybridization potential between the s and d bands is much smaller than chosen.

V. CONCLUSION

We have explained the general behavior of R_H for binary and ternary amorphous Zr-based alloys in terms of the change of λ_{SO}^{SJ}, which depends strongly on the location of ε_F. The estimation of λ_{SO}^{SJ} by correlating $R_H^S \chi_v$ and $\chi_v \rho^2$ illustrated that indeed the behavior of λ_{SO}^{SJ} can be explained qualitatively very well with the density of states near the Fermi level and the band structure observed with UPS spectra. This estimation of λ_{SO}^{SJ} is comparable in magnitude to values estimated for dilute ferromagnetic alloys. The principal difference between the magnitudes of R_H between the two systems is thus due to

the differences in their spin polarizations.

For the ternary alloy system, we explained the increase of R_H for Zr-rich, and a very small increase or even decrease of R_H for Zr-poor Zr-Ni pseudobinary alloys, as a result of the dilution of the Stoner enhancement and its influence on χ_v.

In conclusion, we have argued that the side-jump effect, or the spin-orbit scattering-induced Hall effect, is not negligible, but plays a major role even in purely paramagnetic amorphous alloys. A complicated combination between the resistivity and the spin polarization in conjunction with the band structure provides an explanation of the positive Hall coefficients for the Zr-based amorphous alloys in a completely understandable way. Also, the proposed description provides a coherent and unifying picture for a large number of seemingly discordant observations.

We note that Movaghar and Cochrane[43,44] have questioned the theoretical foundation of the side-jump mechanism. They did not find a side-jump contribution[43] in a tight-binding model calculation of the Hall coefficient based on the Kubo formalism for an amorphous metal, but in the more recent calculation[44] based on consideration of magnetic energy, they found a term with similar properties.

ACKNOWLEDGMENTS

[1]L. Berger and G. Bergmann, in *The Hall Effect and its Applications,* edited by C. L. Chien and C. R. Westgate (Plenum, New York, 1980), p. 55.

[2]T. R. MacGuire, R. J. Gambino, and R. C. O'Handley, Ref. 1, p. 137.

[3]R. Delgado, H. Ambruster, D. G. Naugle, C. L. Tsai, W. L. Johnson, and A. Williams, Phys. Rev. B **34**, 8828 (1986).

[4]P. C. Colter, T. W. Adair, and D. G. Naugle, Phys. Rev. B **20**, 2959 (1979).

[5]M. L. Trudeau and R. W. Cochrane, Phys. Rev. B **39**, 13 212 (1989).

[6]R. W. Cochrane, J. Destry, and M. Trudeau, Phys. Rev. B **27**, 5955 (1983).

[7]M. L. Trudeau, R. W. Cochrane, and J. Destry, Mater. Sci. Eng. **99**, 187 (1988).

[8]B. L. Gallagher, D. Greig, M. A. Howson, and A. M. Croxxon, J. Phys. F **13**, 119 (1983).

[9]A. K. Bhatnagar, R. Pan, and D. G. Naugle, Phys. Rev. B **39**, 12 460 (1989).

[10]K. Rhie, D. G. Naugle, and A. K. Bhatnagar, Z. Phys. B **78**, 411 (1990).

[11]K. Rhie and D. G. Naugle, Phys. Lett. A **149**, 301 (1990).

[12]D. Nguyen-Manh, D. Mayou, G. T. Morgan, and A. Pasturel, J. Phys. F **17**, 999 (1987).

[13]G. F. Weir, W. A. Howson, B. L. Gallagher, and G. J. Morgan, Philos. Mag. **47**, 163 (1983).

[14]M. A. Howson and G. J. Morgan, Philos. Mag. **51**, 439 (1985).

[15]A. Schulte, A. Ekert, G. Fritsch, and E. Lüscher, J. Phys. F **14**, 1877 (1984).

[16]A. Schulte, W. Haensch, G. Fritsch, and E. Lüscher, Phys. Rev. B **40**, 3581 (1989).

[17]L. Berger, Phys. Rev. B **32**, 4559 (1970).

[18]R. W. Cochrane, M. Trudeau, and J. O. Ström-Olsen, J. Appl. Phys. **57**, 3207 (1985).

[19]M. Trudeau, R. W. Cochrane, D. V. Baxter, J. O. Ström-Olsen, and W. B. Muir, Phys. Rev. B **37**, 4499 (1988).

[20]L. Hedman and Ö. Rapp. Phys. Lett. **100A**, 251 (1984).

[21]I. Bakonyi, Phys. Rev. B **45**, 5066 (1992).

[22]The magnetization study near the ferromagnetic transition limit reported that the temperature dependence of the magnetic susceptibility might be caused by superparamagnetic clusters, see Refs. 20 and 21.

[23]K. Rhie, D. G. Naugle, Beomhoan O, and J. T. Markert (unpublished).

[24]I. Kocanović, B. Leotić, J. Lukatela, and J. Ivkov, Phys. Rev. B 42, 11 587 (1990).

[25]A. Tschumi, T. Laubscher, P. Keker, R. Schüpter, H. U. Künzi, and H.-J. Güntherodt, J. Non-Cryst. Solids 61-62, 1091 (1984).

[26]Z. Altounian and J. O. Ström-Olsen, Phys. Rev. B 27, 4149 (1983).

[27]D. Pavuna, J. Non-Cryst. Solids 61-62, 1353 (1984).

[28]H.-J. Eifert, B. Elschner, and K. H. J. Buschow, Phys. Rev. B 25, 7441 (1982).

[29]P. Oelhafen, in Glassy Metals II, edited by H. Beck and H.-J. Güntherodt (Springer-Verlag, New York, 1983), p. 283.

[30]R. Zehringer, P. Oelhafen, H.-J. Güntherodt, Y. Yamada, and U. Mizutani, Mater. Sci. Eng. 99, 253 (1988).

[31]J. Smit, Physica 24, 39 (1958).

[32]R. C. Fivaz, Phys. Rev. 183, 586 (1969).

[33]U. Mizutani, Prog. Mater. Sci. 28, 97 (1983).

[34]G. Busch and H.-J. Güntherodt, Solid State Physics: Advances in Research and Applications, edited by H. Ehrenreich, F. Seitz, and D. Turnbull (Academic, New York, 1974), Vol. 29, p. 235.

[35]V. L. Moruzzi, P. Oelhafen, and A. R. Williams, Phys. Rev. B 27, 2049 (1983).

[36]Y. Yamada, Y. Stoh, U. Mizutani, N. Shibagaki, and K. Tanaka, J. Phys. F 17, 2303 (1987).

[37]Y. Yamada, Y. Itoh, T. Matsuda, and U. Mizutani, J. Phys. F 17, 2313 (1987).

[38]U. Mizutani (private communication). See also Ref. 9.

[39]E. Batalla, Z. Altounian, and J. O. Ström-Olsen, Phys. Rev. B 31, 577 (1985).

[40]U. Mizutani, S. Ohasi, T. Matsuda, K. Fukamitchi, and K. Tanaka, J. Phys. C 2, 541 (1991).

[41]U. Mizutani, Y. Yamada, and C. Mishima, Solid. State. Commun. 62, 641 (1987).

[42]T. A. Stephens, D. Rathnayaka, and D. G. Naugle, Mater. Sci. Eng. A 133, 59 (1991).

[43]B. Movaghar and R. W. Cochrane, Phys. Status Solidi B 166, 311 (1991).

[44]B. Movaghar and R. W. Cochrane, Z. Phys. B 85, 217 (1991).